

Investigations of the optical fields of 3CR radio sources to faint limiting magnitudes – IV

J. E. Gunn^{*}, J. G. Hoessel and J. A. Westphal

*The Hale Observatories, California Institute of Technology, Pasadena,
California 91125, USA*

M. A. C. Perryman^{*} and M. S. Longair^{*}

*Mullard Radio Astronomy Observatory, Cavendish Laboratory, Madingley Road,
Cambridge CB3 0HE*

Received 1980 May 15

Summary. A deep optical survey of the fields of 18 3CR radio sources has been carried out with the Hale 5-m telescope, using a prototype charged-coupled device as a detector. These sources were among the few 3CR objects which were either previously unidentified or associated with very faint images at the plate limit for which confirmation was required.

Ten new identifications are proposed (3C 65, 3C 68.2, 3C 175.1, 3C 239, 3C 241, 3C 267, 3C 272, 3C 289, 3C 469.1 and 3C 470), and candidates for the remaining eight sources are confirmed (3C 34, 3C 61.1, 3C 184, 3C 220.3, 3C 250, 3C 280, 3C 324, 3C 368). Of these identifications, those for 3C 68.2, 3C 175.1, 3C 250 and 3C 470 are considered provisional, since they are displaced from the radio source axes. In addition, the candidate for the 3C 61.1 is classed as a confirmed identification, although the optical field is crowded and an unambiguous identification cannot be made on positional arguments alone.

A subsample of 60 sources from the 3CR catalogue, considered by previous workers, is now (provisionally) completely identified. These new results are used to construct luminosity distributions at $S(178) \geq 20$ Jy and $S(178) \geq 10$ Jy, and the implications of the complete identification rate for models of source evolution formulated by other workers are examined.

1 Introduction

Considerable efforts have been directed towards the detection of the optical counterparts of radio sources from the 3CR catalogue – the work of Kristian, Sandage & Katem (1974, 1978), Longair & Gunn (1975), Smith, Burbidge & Spinrad (1976), Laing *et al.* (1978a), and of Riley, Longair & Gunn (1980) has extended the optical surveys beyond the limit of the Palomar Observatory – National Geographic Society Sky Survey (POSS), in the latter case reaching an estimated 23 mag for certain fields. Even with such high-quality plate

^{*}Present address.

material, numerous faint candidates have required confirmation, and several sources in the statistical sample of 166 3CR radio sources (Jenkins, Pooley & Riley 1977) still remained unidentified.

In this paper, observations of the fields of 18 3CR sources studied inconclusively by Kristian *et al.* (1974, 1978), Laing *et al.* (1978a) and by Riley *et al.* (1980) are described. These sources represent all of those in the complete sample of 166 3CR radio sources for which identifications were absent or required confirmation by deeper plate material, except for the sources 3C 268.1, 3C 294, 3C 322, 3C 356 and 3C 437. The first two fields are obscured by bright stars and were omitted from the current study for this reason.

The observations were made with the Hale 5-m telescope with a prototype charge-coupled device (CCD) as a detector, and are described in Section 2. High-resolution radio maps, obtained with the 5-km telescope with resolution $2 \times 2 \cos \delta \text{ arcsec}^2$ at 5 GHz, have been published for all the sources studied (Pooley & Henbest 1974; Hargrave & McEllin 1975; Longair 1975; Riley & Pooley 1976; Jenkins, Pooley & Riley 1977), and the radio-optical reference frames have been related with an accuracy of better than 1 arcsec in all cases. The reduction procedure used to relate these coordinate systems is described in greater detail in Section 3. The results are presented in Section 4, with positions and magnitudes of the proposed identifications.

2 The optical observations

The observations were made at the prime focus of the Hale 5-m telescope on the nights of 1979 March 2 (3C 280 and 3C 289), March 3 (3C 175.1–3C 272, 3C 324 and 3C 368) and October 17 (the rest) in conditions of good to excellent astronomical seeing. The detector employed was a prototype 500×500 thinned, back-illuminated charge-coupled device (CCD) developed by Texas Instruments as part of a programme sponsored by the US National Aeronautics and Space Administration.

To minimize the dark signal, the CCD was cooled to -120°C by conduction from a liquid nitrogen reservoir; the measured read-out noise is 13 electrons rms, and the full-well capacity is about 50 000 carriers. The pixel size of the array is $15 \times 15 \mu\text{m}^2$, and to couple it efficiently to the $89 \mu\text{m}$ per arcsec scale at the $f/3.52$ prime focus of the 5-m telescope a re-imaging system using a 135-mm $f/2$ Xero-Nikkor and a 55-mm $f/1.2$ Nikkor lens was employed, yielding a pixel size of $0.43 \times 0.43 \text{ arcsec}^2$ and a resultant field 3.6 arcmin square.

The data were digitized to 16-bit accuracy and stored on magnetic tape for subsequent reduction. Real-time display capability was realized by means of a 256×256 6-bit digital scan converter feeding a standard TV monitor.

CCD detectors provide excellent photometric accuracy and linearity (~ 0.1 per cent) over a wide dynamic range (~ 4000 for the device used), and very high responsive quantum efficiencies over a wide spectral range (Antcliffe 1975) – exceeding 60 per cent in the red and near-infrared, where our observations were taken. In addition, the photometric and geometric stability is excellent; the distortions common to electron-optical devices with which such deep identification work has had to deal in the past (Laing *et al.* 1978a) are avoided.

The filters (*i* or *r*) used for the observations were based on the photometric system of Wade *et al.* (1979), an extension of the *uvgr* system of Thuan & Gunn (1976). Transformations to the Johnson *R**I* system are given in Wade *et al.* The system was defined using an S-1 photosurface, whose response shape is sufficiently similar to that of the CCD (albeit more than two orders of magnitude lower!) that there should be little systematic difference.

The infrared exposures were made in order to reduce contamination from the Moon's scattered light, and also to provide information about the spectral region in which the

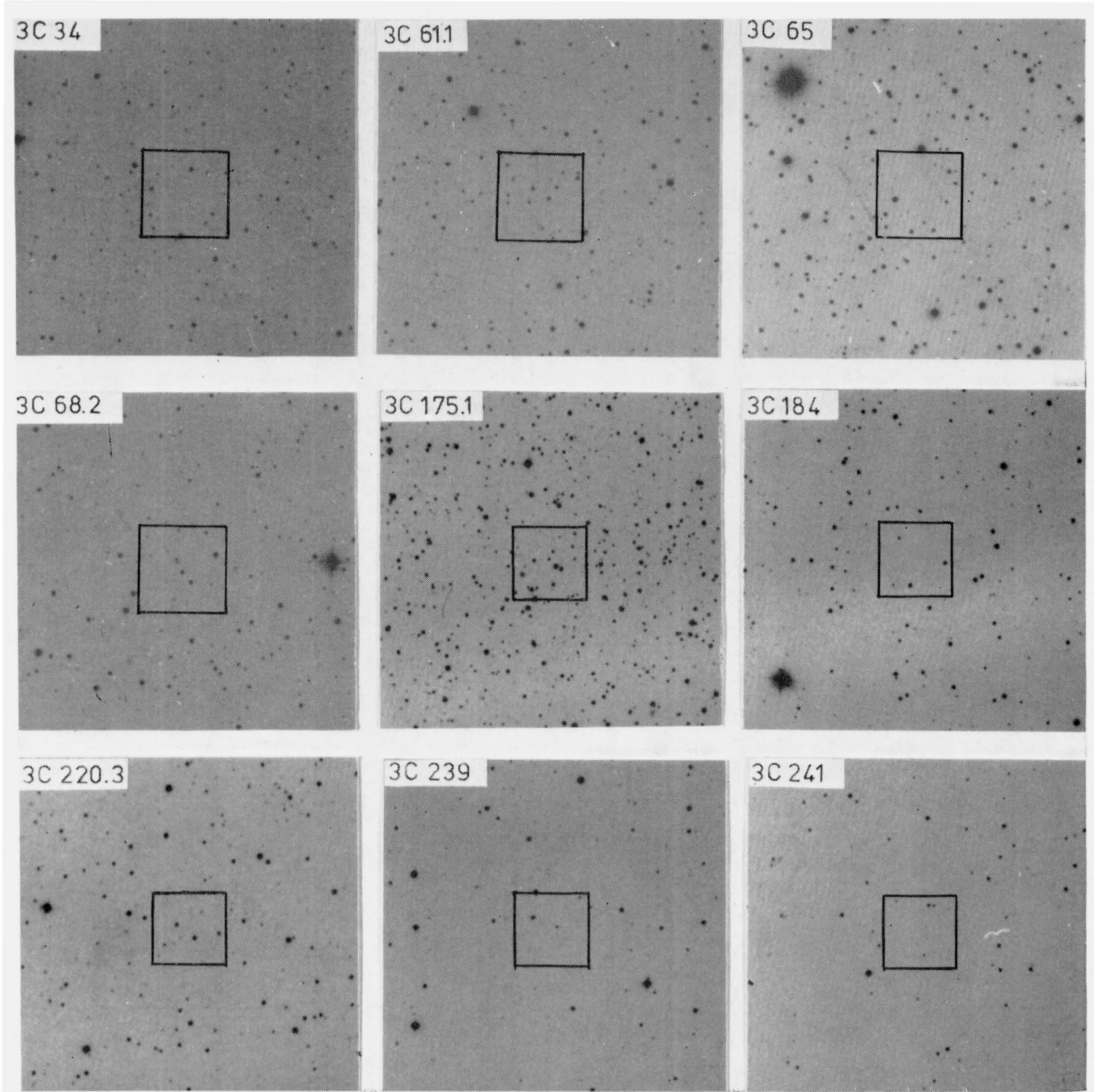


Plate 1. Finding charts for the 18 3CR fields taken from the red prints of the POSS. Each covers an area of 15×15 arcmin², and north is at the top, east to the left. The central boxes indicate the regions of the CCD images displayed as Photowrite images in Plate 2. Copyright by the Palomar Observatory–National Geographic Society Sky Survey. Reproduced by permission from the Hale Observatories.

[facing page 112]

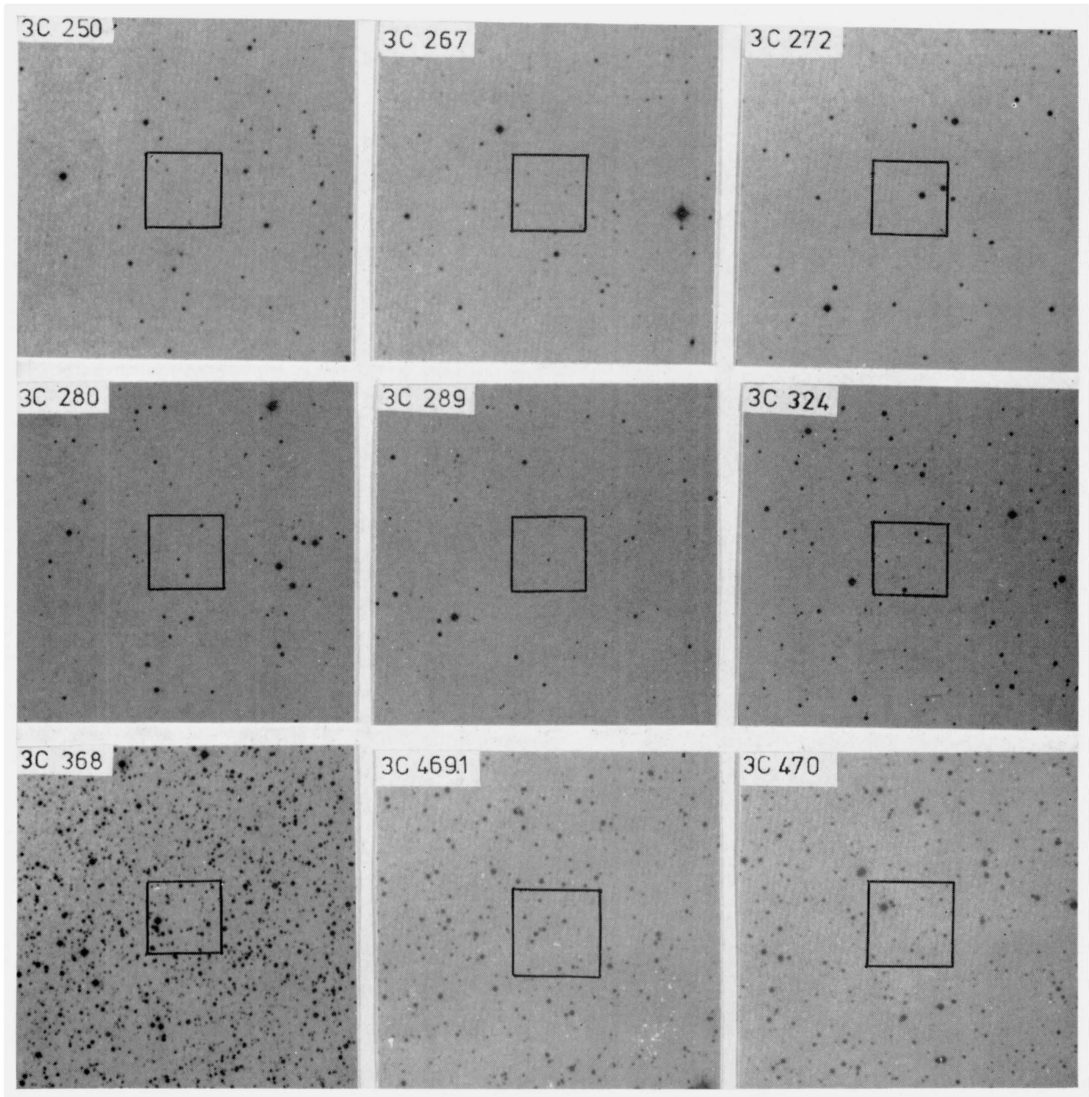


Plate 1—continued

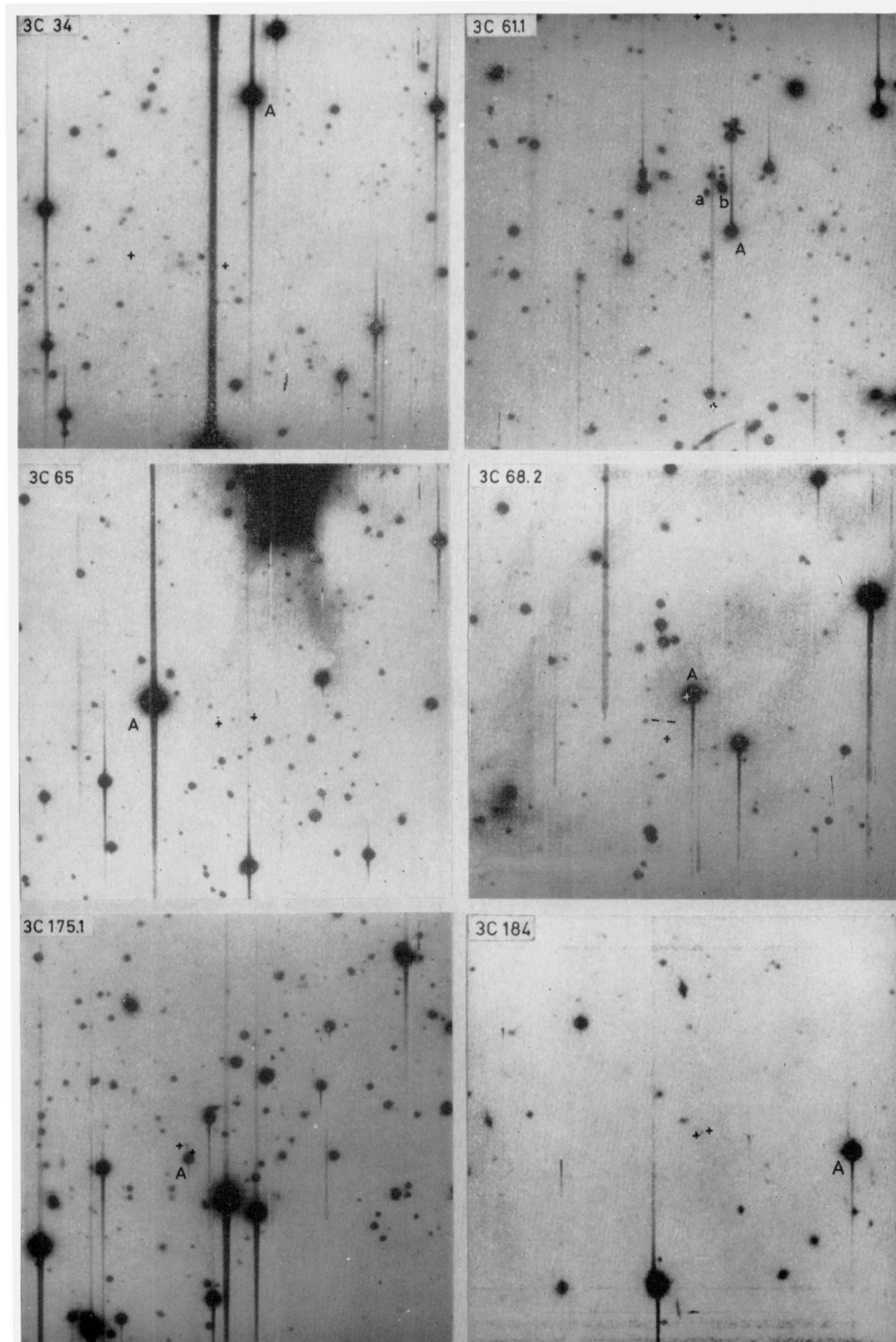


Plate 2. Photowrite images of the calibrated CCD fields. Each covers an area of approximately 3.4×3.4 arcmin². North is at the top, east to the left, and the crosses mark the peaks of the radio brightness at 5 GHz. For each field, the average of all exposures is presented, except for 3C 65 (average of the *i* exposures), 3C 68.2 (average of the *i* exposures), 3C 175.1 (average of *r* exposures), 3C 184 (single *r* exposure only), 3C 220.3 (average of the *r* exposures), and 3C 239 (average of the *i* exposures).

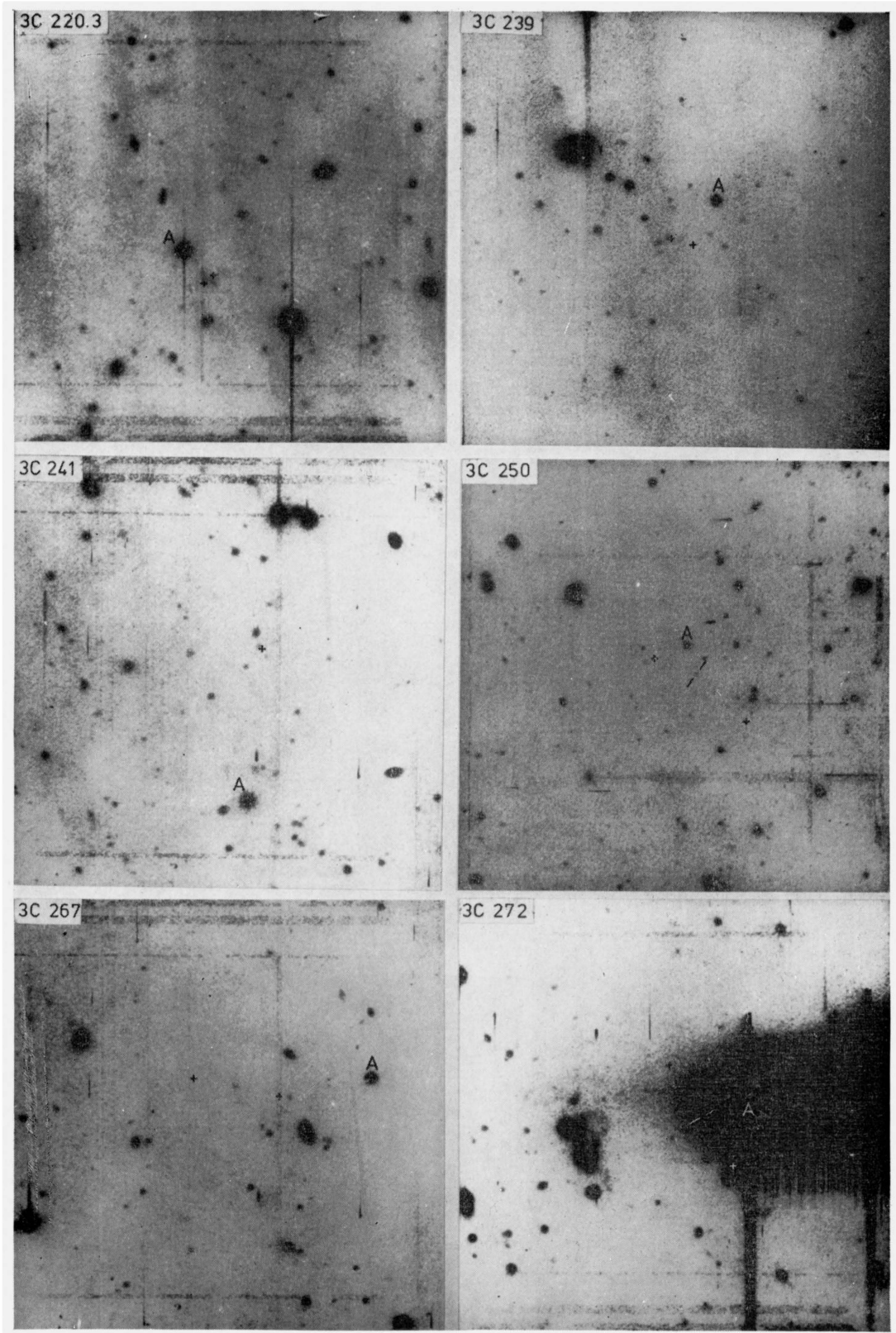


Plate 2—continued

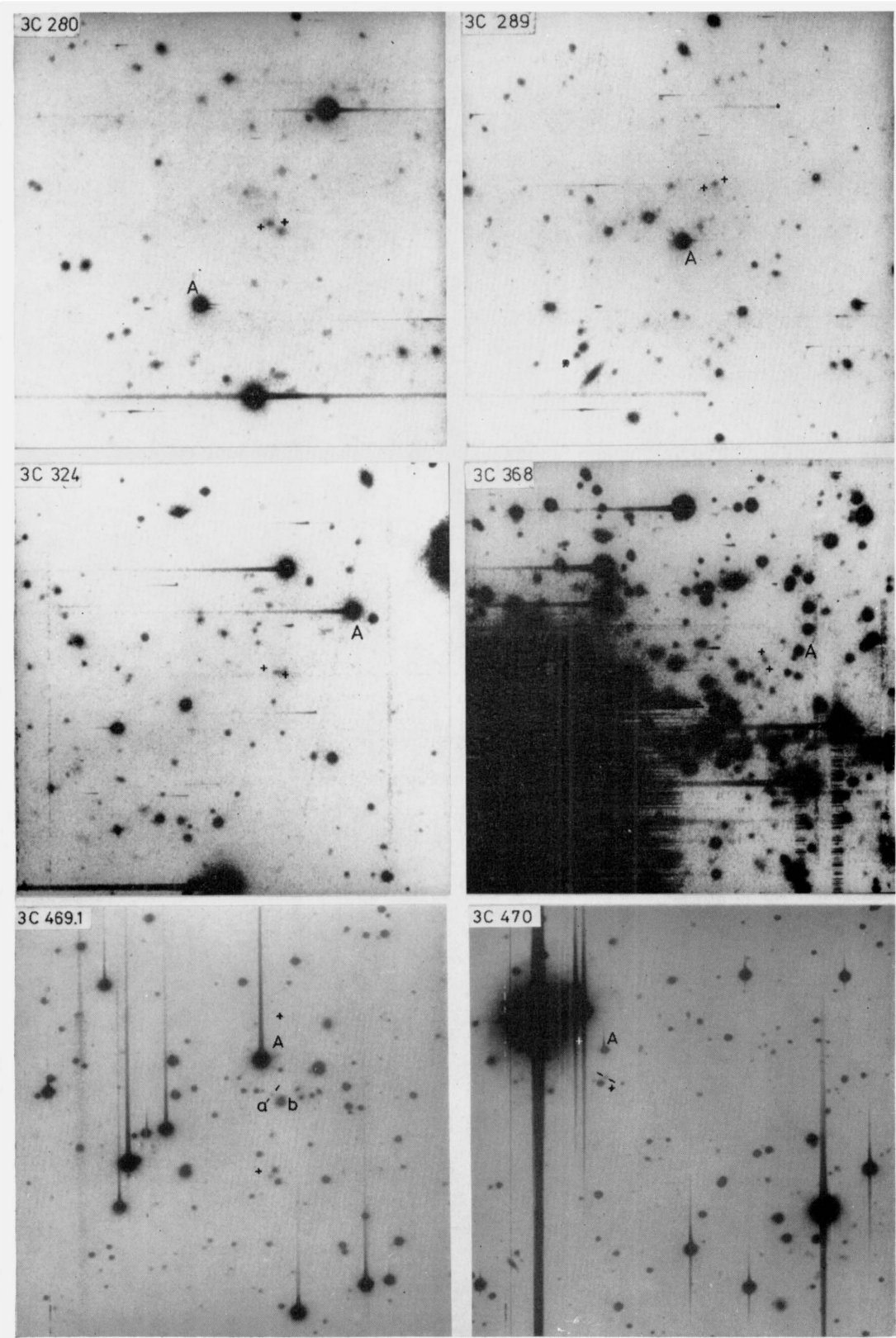


Plate 2—continued

optical emission of giant elliptical galaxies at large redshifts may exceed that in the red. Multiple exposures allowed the reality of faint objects to be confirmed, and discriminated against the effects of possible cosmic-ray events.

3 Analysis of the observations

3.1 REDUCTION OF THE CCD DATA

To provide the maximum number of secondary standard stars for astrometry, the full 500×500 arrays were reduced. As for other two-dimensional detectors, the photometric calibration was performed in two stages:

(i) Relative calibration, or ‘flat-fielding’, to correct for pixel-to-pixel variations in sensitivity across the array. For this purpose a series of zero-exposure frames (giving the intrinsic pixel signal-offsets, as well as an estimate of the read-out noise) and a series of flat-field exposures were taken throughout the night. In principle this allows for any temporal fluctuations in zero-point to be removed, although in practice any such instabilities were dominated by read-out noise, and the final calibration frames used in the photometric reduction were the average of the exposures taken throughout the night. The dark-current generation in the CCD was found to be negligible.

(ii) Conversion of the resulting photometric data into an absolute flux density scale. For this purpose, a series of standard stars were observed and reduced as described above. Their magnitudes in the r and i bands, taken from Wade *et al.* (1979), are given in Table 1. The magnitudes determined for the standards were internally consistent to within the estimated errors, which in all cases are determined by uncertainties in the background level around the source.

Table 1. The standard stars.

Star	Spectral Type	r	i	Exposure (s)	
HD 84937	sd F2	8.39	8.42	5 × 0.5	(1979 March 2 r)
				3 × 0.5	(1979 March 3 r)
				3 × 0.5	(1979 March 3 i)
DM +262606	sd F4	9.75	9.74	1 × 1.0	(1979 March 3 r)
				1 × 1.0	(1979 March 3 i)
HD 19445	sd F7	8.07	8.07	4 × 0.5	(1979 Oct 17 r)
				4 × 0.5	(1979 Oct 17 i)
DM +174708	sd F6	9.50	9.50	6 × 0.5	(1979 Oct 17 r)

Integrated magnitudes for the identifications were determined by subtracting sky background signal, estimated from surrounding empty regions, from the signal over the region of the galaxy. The quoted magnitudes are believed to be accurate to ± 0.5 mag. Although the system should be capable of determining more precise magnitudes, this awaits a more sophisticated algorithm for estimating the excess signal, as well as being dependent on the chosen aperture size.

3.2 ASTROMETRIC REDUCTION

The positions of candidate identifications were determined in two stages, as described by Laing *et al.* (1978a). Prints of the Palomar Observatory–National Geographic Society Survey (POSS) were measured using the x – y measuring machine of the Institute of Astronomy, Cambridge, and the positions of secondary reference stars also visible on the CCD images were determined relative to those of primary positional standards selected from the AGK3

Catalogue using a computer program written by A. N. Argue & P. Stewart. The formal standard error on the precision with which the reference frames were related was always less than 0.4 arcsec.

In the second stage, the positions of the secondary standards and of the candidate identifications were determined from large-scale intensity plots of the photometrically corrected data, and related to the coordinates of the secondary standards measured on the POSS prints using the same regression program. The formal error in determining this reference frame was typically less than 0.2 arcsec. Since the radio and optical reference frames are known to be tied with an accuracy of better than 0.1 arcsec (Elsmore & Ryle 1976), the total error in the relative positioning of the radio and CCD frames of reference is typically less than 0.5 arcsec.

4 Results

4.1 PRESENTATION OF THE RESULTS

To aid the identification of the fields, finding charts taken from the red prints of the POSS are given in Plate 1. Table 2 also gives the RA and Dec (1950.0) of an optical object (A) visible on the POSS red prints near to each radio position. The calibrated CCD fields are presented as Photowrite images in Plate 2. The positions of the peaks of radio brightness at 5 GHz, taken from the references given in Table 2, are indicated by crosses.

Table 2. Details of observations.

3CR	RA (1950.0) dec						5-GHz reference	Previous identification	Exposure (min)	Filter	Magnitude	Identification status
	h	m	s	o	'	"						
34	01	07	30.82	31	31	20.9	JPR	G (RLG)				
			34.39			25.1						
Optical			32.51			21.9			2×10	r	20.7	G
A			29.92		32	38.7						
61.1	02	10	48.8	86	06	41.4	HM	G (LG)				
			41.1		03	35.0						
Optical	'a'		44.1		05	15.8			1×10	r	19.9	G
	'b'		37.1		05	18.5					18.8	G
A			33.9		04	58.2						
65	02	20	36.31	39	47	18.2	L	U (RLG)				
			37.81			15.9						
Optical			37.24			17.1			3×10	r	>23.5	G
									2×10	i	22.3	
A			40.43			27.2						
68.2	02	31	24.38	31	21	21.1	PH	U (KSK)				
			25.12			01.0						
Optical			25.36			10.4			4×10	r	-	G
									2×10	i	23.0	
A			24.25			21.4						
175.1	07	11	14.16	14	41	30.8	JPR	E (KSK)				
			14.60			33.7						
Optical			14.28			33.9			2×10	i	21.0	F0
									2×10	r	22.0	
A			14.30			29.4						
184	07	33	58.41	70	30	02.0	JPR	G (LLRKG)				
			59.25			00.8						
Optical			59.01			01.1			3×5	i	20.9	F0
									1×5	r	22.0	
A			45.44		29	50.7						
220.3	09	31	09.50	83	28	57.1	JPR	G? (LLRKG)				
			12.60			52.4						
Optical			10.46			55.0			2×5	i	21.0	G
									2×5	r	20.8	
A			17.90		29	09.6						
239	10	08	38.29	46	43	06.8	PH	E (LLRKG)				
			39.33			09.8						
Optical			38.97			08.4			2×5	i	21.5	G
									2×5	r	22.5	
A			37.36			26.5						
241	10	19	09.36	22	14	39.5	JPR	E (LLRKG)				
			09.44			40.7						
Optical			09.87		13	30.8			2×15	r	22.6	F0
A												

Table 2 – continued

3CR	RA (1950.0) h m s	dec ° ' "	5-GHz reference	Previous identification	Exposure (min)	Filter	Magnitude	Identification status
250	11 06 09.67	25 16 55.5	JPR	G (LLRKG)				
Optical	12.56	17 25.0						
A	11.31	17 18.3			1×15	r	22.8	F0
	11.61	17 31.5						
267	11 47 20.87	13 03 55.7	JPR	G? (LLRKG)				
Optical	23.40	04 02.5						
A	22.11	04 00.2			1×15	r	22.1	G
	17.98	04 03.0						
272	12 21 59.53	42 22 44.5	JPR	E (KSK)				
Optical	22 01.77	23 36.0						
A	00.88	13.3			1×15	r	23.0	F0
	21 58.82	23 25.0						
280	12 54 40.78	47 36 32.2	PH	F0 (KSK)				
Optical	42.05	32.0						
A	41.66	32.7			2×15	r	21.5 (21.6)	Stellar ? G
	(41.10	29.1)						
	44.78	35 56.5						
289	13 43 26.91	50 01 33.9	JPR	E (KSK)				
Optical	27.90	30.7						
A	27.38	32.0			2×15	r	23.0	G?
	29.03	05.6						
324	15 47 36.82	21 34 39.6	JPR	G? (KSK)				
Optical	37.53	42.5						
A	37.10	40.1			1×15	r	22.1	F0
	34.63	35 06.8						
368	18 02 45.55	11 01 09.6	JPR	G? (LLRKG)				
Optical	45.72	17.9						
A	45.60	13.8			1×15	r	21.6	F0
	44.54	17.5						
469.1	23 52 56.92	79 39 12.1	L	G (LG)				
Optical	53 01.16	37 58.9						
A	'a' 52 58.67	38 35.2			1×10	r	22.7	F0
	53 00.38	38 51.7						
470	23 56 02.30	43 47 56.2	RP	U/G(RLG)				
Optical	03.66	48 15.0						
A	02.50	47 59.8			3×10	r	22.5	F0
	02.57	48 12.4						
HM	Hargrave & McEllin (1975)		KSK	Kristian, Sandage & Katem (1974)				
JPR	Jenkins, Pooley & Riley (1977)		LLRKG	Laing et al. (1978a)				
L	Longair (1975)		LG	Longair & Gunn (1975)				
PH	Pooley & Henbest (1974)		RLG	Riley, Longair & Gunn (1980)				
RP	Riley & Pooley 1976)							

The Photowrite images of the reduced CCD data were produced using a linear density-scale ranging from white at a lower bound of 0.5σ above the mean background level, to black at an upper bound of about 10σ above the background. In the cases where multiple exposures of the same field were taken (see Table 2), no evidence was found for spurious images (for example, due to particle events) appearing in the fields, apart from faint ‘ghost’ images near to very bright stars. The vertical or horizontal striations appearing on the images are artefacts of the detector, and are due to charge overflow at saturated pixels (‘blooming’), to persistence of previous images, or to defective pixel columns due to faults in chip manufacture. For presentation purposes, the striations which recurred on independent images were removed by linear interpolation across the affected columns – this has little effect on the real data since the image is somewhat oversampled. In cases where these striations passed through the identification, corrections were determined from similarly affected regions surrounding the object. The Mk II chip, used for the October observations, suffered less noticeably from such defects. Small residual background variations show up as blotches on the CCD images.

A problem with the images taken on October 7 (3C 34, 61.1, 65, 68.2, 175, 469.1, 470) is that ghost images of the brightest stars in the field are present. These were due to reflection off the filter. We have made no attempt to remove these spurious images but urge caution in the interpretation of the images. The ghosts appear as ‘stars’ or ‘galaxies’ located

at the point of reflection symmetry about the centre of the field. Thus, for example, the 'star' to the north of star A in 3C 34 is the ghost of the bright star at the bottom of the frame. We have inspected the fields carefully to determine whether our conclusions are affected by this problem and are confident that none of our proposed identifications are ghosts.

The details of the observations and the results are presented in Table 2, where the columns are arranged as follows:

- 1 3CR number.
- 2 and 3 Right ascension and declination (1950.0 coordinates are used throughout) of the peaks of the radio emission, and of the optical candidate as determined above. For each field, 'A' is a nearby optical object visible on the red prints of the POSS.
- 4 Reference to the structure at 5 GHz.
- 5 Previous identification status and observers. E signifies an empty field, G a galaxy, FO a faint object.
- 6 Number of exposures, and exposure time.
- 7 Filter.
- 8 Integrated apparent magnitude of the candidate identification.
- 9 Current identification status.

4.2 NOTES ON INDIVIDUAL SOURCES

3C 34. Confirmed identification. The radio source is an asymmetric double with components separated by 48 arcsec. Kristian *et al.* (1978) proposed that the possible variable 19.5-mag stellar object 4 arcsec off the radio source axis towards the western (weaker) component was a quasar candidate. The observations of Riley *et al.* (1980) revealed a diffuse object with an estimated integrated magnitude of about 20.5 lying between the components of the double source. Our present CCD observations confirm the reality of this object, and, although no central component of the radio source has been detected, the positional coincidence of our candidate with the mid-point of the components makes this object a certain identification. It is, in addition, distinctly elliptical with a diffuse envelope whose major axis is coincident with the axis of the double source, and faint cluster members are clearly visible in our images. Our integrated magnitude of 20.7 in *r* agrees well with the estimates of Riley *et al.* (1980).

3C 61.1. Confirmed identification. The radio source is a 185-arcsec double along p.a. $2^\circ.5$ (Hargrave & McEllin 1975). Although a large fraction of the radio flux originates in an extensive bridge of emission, there is no central component and an unambiguous identification has yet to be claimed. Successive optical studies (Shakeshaft & Longair 1965; Wyndham 1966; Longair & Gunn 1975) have revealed an extended cluster of galaxies including a blue stellar object (Penston 1971) at redshift of 0.184 (Miller, Robinson & Wampler 1973). The most recent deep plates of Longair & Gunn (1975) and Kristian *et al.* (1978) have not revealed any further candidates nearer to the mid-point of the double source.

The 'triplet of galaxies' first noted by Shakeshaft & Longair (1965) shows up in our present image as a tight grouping of five objects, 35 arcsec to the west of the blue stellar object. Kristian *et al.* (1978) favour the brightest of the original three galaxies (to the south-east of the association) as the most likely identification. This galaxy, 'a' on our CCD image, is only 8 arcsec from the mid-point of the double and lies on the source axis, although object 'b', 13 arcsec from the mid-point and about 8 arcsec from the source axis, now appears to be the dominant galaxy – our image, reaching a lower surface brightness, indicates a possible cD morphology.

Our measurement of the secondary standard stars favours the positions given by Longair & Gunn (1975) rather than those of Kristian *et al.* (1978) although, as the latter point out, the discrepancy of 2 arcsec in RA and Dec does not affect the identification status. With a radio component separation of 185 arcsec neither of the above candidates can be dismissed on the grounds of positional coincidence, and confirmation must await an improved radio map or spectroscopy of the candidates.

3C 65. New identification. The radio source is an equal double with a component separation of 17.4 arcsec (Longair 1975). The optical field has been well studied (Kristian *et al.* 1974; Longair & Gunn 1975; Riley *et al.* 1980) with no candidate identification revealed. On each of our 10-min exposures in *r* a very faint object is just detected at the mid-point of the double source. However, the object is prominent on each of the *i* exposures, and appears extended. Our *i* magnitude of 22.3 and our lower limit of $m_r > 23.5$ make it a similar object to the identifications found for 3C184 and 3C 239, where a significantly larger flux density is detected in the *i* band. Before our October observations Grasdalen (1980) reported the detection of the optical counterpart to 3C 65 in the 2.2- μ m band, and has drawn attention to this steep-spectrum behaviour.

3C 68.2. New identification? The radio source is a symmetric double with components separated by 22 arcsec (Pooley & Henbest 1974). The Np component is almost coincident with the image of a bright star. This object was originally proposed as the optical counterpart (Wyndham 1966) although it was subsequently shown to be a star (see Macdonald, Kenderdine & Neville 1968). Like 3C 65 this has been a particularly stubborn field, and the work of Kristian *et al.* (1974), Longair & Gunn (1975), Smith *et al.* (1976), and Riley *et al.* (1980) failed to provide a further candidate.

Again our CCD image reveals nothing in *r*, but a candidate is clearly visible on both 10-min exposures in *i*, with $m_i = 23.0$. Our candidate, however, lies 8 arcsec from the mid-point of the double off the radio-source axis. Its steep spectral behaviour in the optical may argue in favour of it being the optical counterpart – and occasional asymmetry in the position of the identification is not unknown (see Section 5). The true identification status therefore awaits deeper fields or spectroscopic studies.

3C 175.1. New identification? The region between the radio components of the 7-arcsec double was originally partly obscured by a row of defective pixels. A 21-mag object lies about 1.5 arcsec from the mid-point of the radio source, and the reality of this object was confirmed by a further CCD image of the field taken with the *r* filter during the October run (Plate 2). ‘A’ is an 18-mag blue stellar object 3 arcsec from the centre of the double, our position agreeing with that given by Jenkins *et al.* (1977). Spectroscopic observations by C. R. Lynds (private communication) have shown this to be a star, and no other objects were detected by Kristian *et al.* (1974).

3C 184. The faint galaxy noted by Laing *et al.* (1978a) is confirmed. Our position lies less than 1 arcsec from the mid-point of the 4.4-arcsec double, and the object is about 1 mag brighter in the *i* band than in the *r*.

3C 220.3. A very diffuse object lies between the components of this 7.4-arcsec double. We classify this as a confirmed identification, although object B of Laing *et al.* is not obviously a real detection, and bears little resemblance to the extended object found here. The spectrum is flat between the *r* and *i* bands. The complex optical morphology of the candidate requires further investigation. It lies in a cluster of galaxies of which it is by far the brightest, suggesting that it may be a cD galaxy.

3C 239. New identification. Nothing was seen at this position on the good 5-m plate of Laing *et al.* The radio source is an asymmetric 11.2-arcsec double, and the new identification lies on the source axis, 4 arcsec from the brighter N_f component. The object is, like 3C 184, about 1 mag brighter in the *i* band than in the *r*. Several other nearby objects not present on the 5-m plate are also detected. These may be members of an associated cluster.

3C 241. New identification. This was an empty field on the good 5-m plate of Laing *et al.* The radio source is unresolved at 15 GHz, and our optical position agrees to within 1 arcsec in RA and Dec with that of the radio component. The bright object 10 arcsec north is the object noted by Laing *et al.*

3C 250. 'Confirmed' identification. The object listed by Laing *et al.* is not seen on our CCD image; our nearest object, which was also noted by Laing *et al.*, lies about 3 arcsec from the radio source axis, although it is 8 arcsec from the mid-point of the 49-arcsec double. In view of this potential discrepancy, the identification should be regarded as provisional.

3C 267. New identification. The diffuse object noted by Laing *et al.* was in a region badly confused by noise. Our CCD image shows that this object is not real, but there is a galaxy about 1 arcsec from the midpoint of the asymmetric 38-arcsec double. There is another faint object 7 arcsec south of the identification.

3C 272. New identification. The field lies in the halo of a bright star about 15 arcsec to the west. Our position for the proposed identification lies about 3 arcsec in right ascension and declination from the centre of the 59-arcsec double, although there is a relatively large uncertainty in defining the CCD coordinate system because of the small number of secondary stars that can be used in the fit.

3C 280. The positions of the two faint objects noted by Kristian *et al.* (1974) are confirmed. The most probable identification lies on the axis of the 12.9-arcsec double, 4 arcsec from the fainter (following) component. This object is apparently stellar, whereas the other object listed in parentheses in Table 2 (off the source axis) is certainly extended.

3C 289. New identification. This extended object lies about 0.3 arcsec from the mid-point of the 10-arcsec double.

3C 324. Confirmed identification. The object proposed by Kristian *et al.* (1974) is the fainter of two objects separated by 3 arcsec, and is about 1 arcsec from the mid-point of the 10-arcsec asymmetric double. Neither object was noted by Laing *et al.* on their 4-m plate.

3C 368. The possible identification noted by Laing *et al.* is confirmed. This is the brighter of two objects 2 arcsec apart, and lies about 0.5 arcsec from the mid-point of the 9-arcsec double.

3C 469.1. New identification? The radio source is a 74-arcsec double (Longair 1975). Longair & Gunn (1975) drew attention to the presence of several galaxies having $m_v \sim 21$ within 10 arcsec of the source axis, suggesting the presence of a distant cluster. Our CCD image reveals numerous objects near to the mid-point, of which 'a' is only 1 arcsec from the mid-point with $m_r = 22.7$. Object 'b' is a ghost image, and a further CCD image is required to confirm the present findings.

3C 470. New identification? The radio source is a 24-arcsec double (Riley & Pooley 1976). Riley *et al.* (1980) suggest a possible very faint object approximately 1 arcsec from the source axis, displaced towards the northern component. This is not confirmed by our

present observations, but there is an object on the source axis, 6 arcsec from the mid-point nearer to the south component, with $m_r = 22.5$. The identification should therefore be regarded as provisional.

5 Discussion

Of the 18 fields studied here, 10 have new proposed identifications, and the remaining 8 have faint objects already proposed as identifications by previous workers now confirmed. Our positions for the faint galaxy proposed by Laing *et al.* for the identification of 3C 220.3 is in better agreement with that of the radio centre. In the cases of 3C 65, 3C 68.2, 3C 175.1, 3C 184 and 3C 239, appreciably more flux is detected in the infrared band than in the red; the integrated magnitudes in the two bands do not differ significantly in the case of 3C 220.3; in all other cases observations were confined to one filter. These results suggest that these are very distant galaxies in which the galaxy spectrum is almost wholly redshifted into the infrared waveband. The faint objects claimed as possible identifications are generally diffuse and therefore probably galaxies. Four of the proposed identifications are displaced from the radio centroid (3C 61.1, 3C 175.1, 3C 250 and 3C 470) and require further confirmation. Significant displacement of the identification from the radio centroid is occasionally

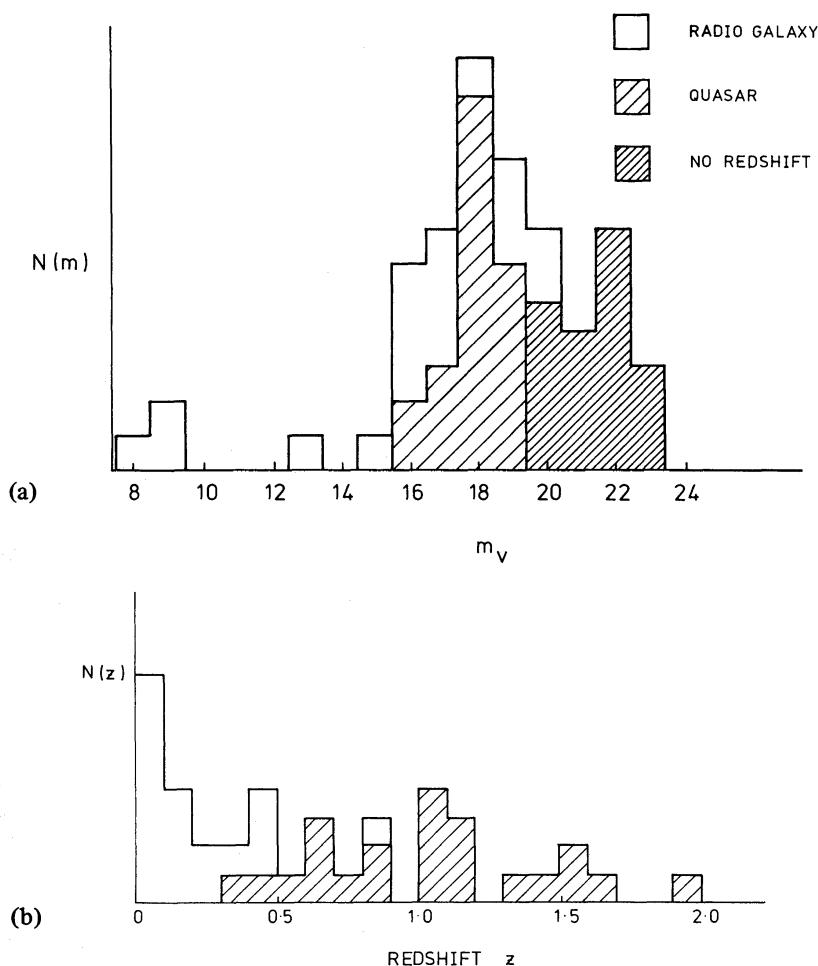


Figure 1. (a) The apparent magnitude distribution for the complete subsample of 60 3CR radio sources, all of which now have optical identifications. (b) The redshift distribution for this sample. Redshifts are only available for 41 of these sources, the apparent magnitudes of those with unknown redshifts are indicated in (a).

observed, however — the quasars 3C 270.1 and 3C 275.1 are examples of such behaviour, and Harris (1974) has drawn attention to the smaller misalignments frequently found between radio lobes and the optical identification.

Due partly to the differing galactic latitudes, the density of optical objects over the fields varies considerably. But the average surface density of objects is about 2×10^{-3} per square arcsec, and the corresponding *a priori* probability for finding an object within a search area of 1 arcsec of the radio centre is less than 1 per cent. In most cases then, the probability of a misidentification due to a chance coincidence of a spurious background object (or of a particle event in the case of the single exposures of 3C 61.1, 3C 272, 3C 324 and 3C 469.1) is very small. A more detailed investigation is required to determine whether the candidates observed to lie significantly displaced from the radio centroid are true identifications.

Despite the fact that some radio galaxies should presumably be too distant to be observed optically at present, this preliminary investigation using a CCD detector of the fields of some of the brighter radio sources has been very successful. In particular, for the 60-source subsample selected by Laing *et al.* (1978b), we can now claim an identification rate of between 98–100 per cent — depending on whether 3C 250 is considered to be correctly identified (the other identifications significantly displaced from the radio centroids are not in this subsample). Fig. 1(a) shows the apparent magnitude distribution for this 60-source sub-

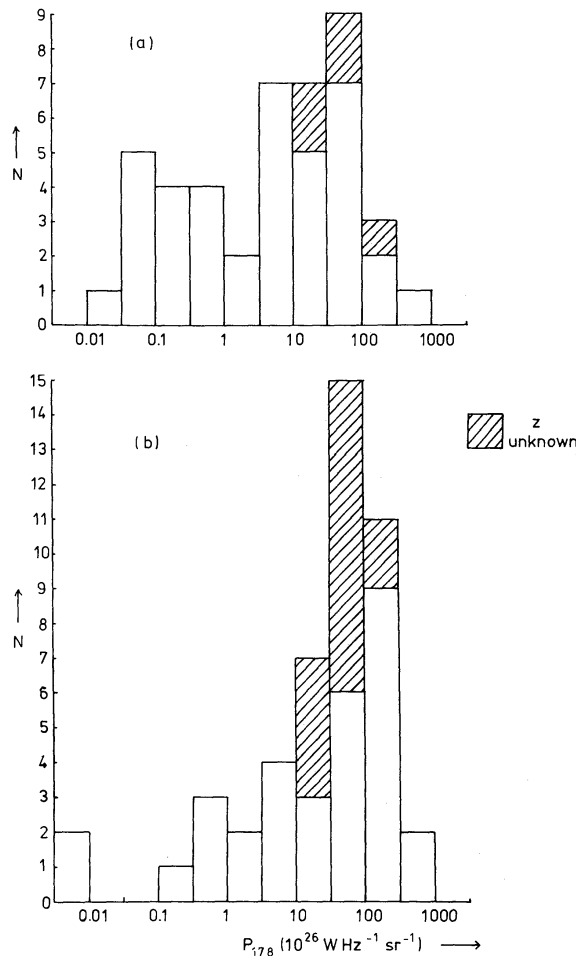


Figure 2. The luminosity distributions for (a) the 43 sources with $S(178) \geq 20$ Jy, and (b) for the 47 sources in the 60-source subsample of Laing *et al.* (1978b) with $20 \geq S(178) \geq 10$ Jy. Luminosities for sources with unknown redshifts were estimated from their apparent magnitudes, and are shown shaded. The calculations are for the geometry $\Omega = 0$, and $H_0 = 50 \text{ km s}^{-1} \text{ Mpc}^{-1}$.

sample. Fig. 1(b) shows the redshift distribution for the 41 sources with known redshifts from this subsample.

Luminosity distributions are presented for two independent source samples. Fig. 2(a) shows the luminosity distribution for the 43 sources from the 166 sample with $S(178) \geq 20$ Jy, determined for the geometry $\Omega = 0$, with $H_0 = 50 \text{ km s}^{-1} \text{ Mpc}^{-1}$. Shaded boxes indicate the five sources in this sample for which redshifts are unknown – values of z between 0.6–1.0, estimated from their apparent magnitudes, were assigned to these sources. Fig. 2(b) shows the corresponding distribution for the 47 sources from the 60-source subsample with $20 > S(178) \geq 10$ Jy. Fifteen of these sources have undetermined redshifts, and their estimated luminosities are again shown shaded. Essentially all of these sources are radio galaxies and hence, although there is some uncertainty in the estimated redshift, the uncertainty in the radio luminosity is relatively small and cannot affect our conclusions about the overall shape of the luminosity distribution. The increasing contribution of high-luminosity sources in the lower flux density interval is very pronounced – this enhancement of the high-luminosity component, also inferred from the values of V/V_{max} for identified sources, is a common feature of evolution functions proposed to explain the behaviour of low-frequency source counts.

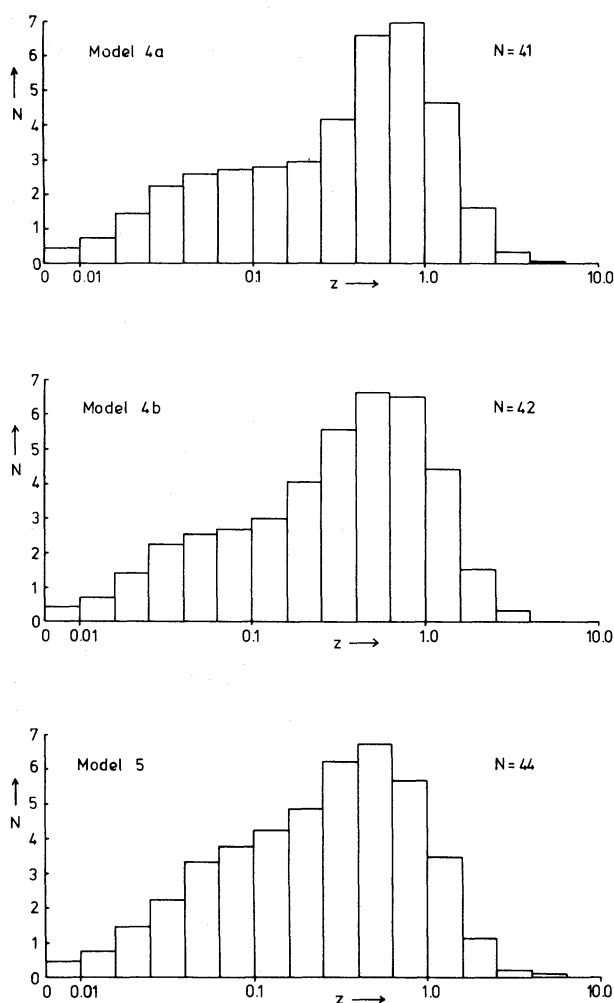


Figure 3. The predicted redshift distributions for the flux density interval $18.6 > S(178) > 10.0$ Jy for models 4a, 4b & 5 from Wall *et al.* (1977). The luminosity distribution defining the parent population is the $S(408) \geq 10$ Jy sample of Wall *et al.*

From an extrapolated magnitude–redshift diagram for the identified sources with known redshifts from the 3CR complete sample, it would appear that $z \leq 1.6$ for $m \leq 23$. Some uncertainties will arise from extrapolation of our integrated red magnitudes into the visual, but it is evident that only a very small percentage of sources with $S(178) \geq 10$ Jy will have redshifts larger than about 1.6. This, in turn, places constraints on the upper end of the luminosity function of radio galaxies at large redshifts, and models of source evolution must be consistent with such a high identification rate for samples selected at high flux densities. We have taken the luminosity distribution of Wall, Pearson & Longair (1977), defined by $S(408) \geq 10$ Jy, and, assuming a low-frequency spectra index of 0.75 for all sources, constructed a corresponding parent sample complete to $S(178) \geq 18.6$ Jy. The predicted redshift distributions for a sample with $S(178) \geq 10$ Jy have then been calculated using this luminosity distribution and the evolution models with optimized parameters taken from Wall *et al.* (models 4a, 4b and 5 in their notation). These predicted distributions are shown in Fig. 3, normalized to a solid angle of one steradian. The expected numbers of sources in the subsample of Laing *et al.* with $z \geq 1.6$ are 2.8, 2.7 and 2.0 respectively.

Although these observations are therefore unable to discriminate between the predictions of such models, they are certainly consistent with the form of the luminosity function predicted at large redshifts by these examples of luminosity-dependent density evolution. Since the source counts diverge most strongly from the Euclidean expectation over just this flux density range, the results are nevertheless encouraging – colours and redshifts of these faint identifications are required to place firmer constraints on the form of the cosmological evolution of the radio source population.

Finally, the association of these remaining 3CR fields with distant galaxies has a further interesting implication. The ‘local-hole’ hypothesis (e.g. Kellermann 1972) is certainly no longer tenable – the steep initial rise observed in the source counts is due to sources optically identified with distant galaxies, and the surrounding deficit of bright radio sources therefore extends out to cosmological distances.

Acknowledgments

We thank M. A. Carr, R. Lucinio, V. E. Nanow and J. D. Smith for indispensable aid in the construction of the instrument; D. M. Odell, D. J. Titterton and P. J. Warner for help in the data reduction; the Director of the Institute of Astronomy for the use of the x – y measuring machine; and E. J. Kibblewhite and T. A. Hooley for the use of their plate-scanning presentation facilities. We thank the Director of the Hale Observatories for observing privileges on the 5-m telescope, and we are particularly grateful to the members of the Wide Field Camera Team of the Space Telescope Project for permission to use their CCD detector for this programme. J. M. Riley kindly provided precise secondary standard positions for the sources studied in Paper III. MACP acknowledges the receipt of a maintenance award from the SRC.

References

- Antcliff, G. A., 1975. *Texas Instruments Report 08-75-41*.
- Elsmore, B. & Ryle, M., 1976. *Mon. Not. R. astr. Soc.*, **174**, 411.
- Grasdalen, G., 1980. *IAU Symp. 92: Objects at Large Redshifts* eds. Abell, G. O. and Peebles, P. J. E., Reidel, Dordrecht, in press.
- Hargrave, P. J. & McEllin, M., 1975. *Mon. Not. R. astr. Soc.*, **173**, 37.
- Harris, A., 1974. *Mon. Not. R. astr. Soc.*, **166**, 449.
- Jenkins, C. J., Pooley, G. G. & Riley, J. M., 1977. *Mem. R. astr. Soc.*, **84**, 61.

- Kellermann, K. I., 1972. *Astr. J.*, **77**, 531.
- Kristian, J., Sandage, A. & Katem, B., 1974. *Astrophys. J.*, **191**, 43.
- Kristian, J., Sandage, A. & Katem, B., 1978. *Astrophys. J.*, **219**, 803.
- Laing, R. A., Longair, M. S., Riley, J. M., Kibblewhite, E. J. & Gunn, J. E., 1978a. *Mon. Not. R. astr. Soc.*, **183**, 547.
- Laing, R. A., Longair, M. S., Riley, J. M., Kibblewhite, E. J. & Gunn, J. E., 1978b. *Mon. Not. R. astr. Soc.*, **184**, 149.
- Longair, M. S., 1975. *Mon. Not. R. astr. Soc.*, **173**, 309.
- Longair, M. S. & Gunn, J. E., 1975. *Mon. Not. R. astr. Soc.*, **170**, 121.
- Macdonald, G. H., Kenderdine, S. & Neville, A. C., 1968. *Mon. Not. R. astr. Soc.*, **138**, 259.
- Miller, J. S., Robinson, L. B. & Wampler, E. J., 1973. *Astrophys. J.*, **179**, 183.
- Penston, M. V., 1971. *Astrophys. J.*, **170**, 395.
- Pooley, G. G. & Henbest, S. N., 1974. *Mon. Not. R. astr. Soc.*, **169**, 477.
- Riley, J. M., Longair, M. S. & Gunn, J. E., 1980. *Mon. Not. R. astr. Soc.*, **192**, 233.
- Riley, J. M. & Pooley, G. G., 1976. *Mem. R. astr. Soc.*, **80**, 105.
- Shakeshaft, J. R. & Longair, M. S., 1965. *Observatory*, **85**, 30.
- Smith, H. E., Burbidge, E. M. & Spinrad, H., 1976. *Astrophys. J.*, **210**, 627.
- Thuan, T. X. & Gunn, J. E., 1976. *Publs astr. Soc. Pacif.*, **88**, 543.
- Wade, R. W., Hoessel, J. G., Elias, J. H. & Huchra, J. P., 1979. *Publs astr. Soc. Pacif.*, **91**, 35.
- Wall, J. V., Pearson, T. J. & Longair, M. S., 1977. In *IAU Symp. 74: Radio Astronomy and Cosmology*, ed. Jauncey, D.
- Wyndham, J. D., 1966. *Astrophys. J.*, **144**, 459.